The silencing of *TdIPK1* genes enhances micronutrient concentration in durum wheat grain

Arianna Frittelli [a], Samuela Palombieri [a], Giulia Quagliata [a], Silvia Celletti [a], Stefania Astolfi [a], Ermelinda Botticella [b], Stefania Masci [a], Pasquale De Vita [c], Mirko Volpato [d], Francesco Sestili [a,*]

[a] *Department of Agriculture and Forest Sciences, University of Tuscia, Via S. Camillo de Lellis, SNC, Viterbo 01100, Italy*
[b] *Institute of Sciences of Food Production (ISPA) – CNR, Via Provinciale Lecce-Monteroni, Lecce 73100, Italy*
[c] *Council for Agricultural Research and Economics, Research Centre for Cereal and Industrial Crops (CREA-CI), S.S. 673, Km 25,200, Foggia 71122, Italy*
[d] *Grandi Molini Italiani, Via Elettricità, 13, Venezia 30175, Italy*

ARTICLE INFO

ABSTRACT

Phytic acid (PA) is the main storage form of phosphorus in kernel and is considered an anti-nutritional compound because of its ability to bind to essential minerals such as iron (Fe), zinc (Zn), potassium (K), calcium (Ca) and magnesium (Mg), thus limiting their availability, especially for populations whose diet is largely based on staple crops.

This study reports a promising nutrient biofortification approach of durum wheat. The approach was based on the silencing of the gene encoding the *inositol pentakisphosphate 2- kinase 1* (*IPK1*), involved in the last step of the PA biosynthetic pathway, through a Targeting Induced Local Lesions IN Genomes (TILLING) approach. Single knockout mutants for the *IPK1* homeoalleles were identified and crossed to pyramid the two mutations. Although an elevated number of plants (F$_2$ and F$_3$ progenies) were analysed, no genotypes lacking both the homeoalleles were recovered, suggesting that the expression of *IPK1* is crucial for seed formation in the spike and/or for plant germination and development.

The characterization of the single null genotypes highlighted that the partial TdIPK1-B1$^-$ mutants showed a lower accumulation of PA in the kernel along with a higher content of essential microelements (Fe, Mn, Zn) compared to the control wild-type. The pattern of mineral accumulation was different for the TdIPK1-A1$^-$ mutants which only presented a greater accumulation of K.

1. Introduction

Over the past decade, the international research community has faced challenges in reducing malnutrition, often referred to as the 'triple burden of malnutrition', including overnutrition, undernutrition and micronutrient deficiencies.

In 2015, the countries of the United Nations committed to the 2030 Agenda for Sustainable Development, with the aim to eliminate all forms of malnutrition and guarantee that all people have access to safe, nutritious and sufficient food [1].

Micronutrient malnutrition, or hidden hunger, is one of the major impediments to proper growth, development, and overall health, and usually results from inadequate intake of vitamins and minerals due to poor diet, limited food availability or reduced absorption [2].

The Food and Agriculture Organization (FAO) estimates that 11 % of

the current world population is suffering extreme food shortages, and 17 % suffers from micronutrient deficiencies [3].

Therefore, micronutrient deficiencies affect 3 billion people, resulting in deleterious impacts on human health especially in low- and middle-income countries with already high levels of food insecurity mainly due to staple crops-based diets [4]. Although these crops can satisfy the daily caloric requirement, they do not provide the right quantities of essential nutrients required for the maintenance of optimal health, physiological function and well-being [5–7].

The most common micronutrient deficiencies include iron (Fe), zinc (Zn), iodine (I) and vitamins deficiency and affect especially women and children by weakening the immune system, leading to infections such as diarrhea, stunting, blindness, anemia, fetal malformations and developmental difficulties. For these reasons, they are a serious health, economic and social concern in vulnerable countries.

Over time, different strategies have been employed to improve micronutrient intake, including diet supplementation, fortification and diversification [8]. Each of these interventions can bring benefits, but all have limitations depending on the context and available resources.

Supplementation programs have been developed to address deficiencies in iron [9,10] and zinc [11,12]. However, supplementation is often considered unpractical for its short-term nature, high costs and challenges in reaching vulnerable populations.

Food fortification consists in the approach of raising the content of one or more micronutrients in food to improve the nutritional quality providing public health benefits. Despite its potential, food fortification faces challenges due to a lack of national laws; moreover, fortification projects tend to favour metropolitan areas and places with greater socioeconomic standing than rural areas [13,14].

Another strategy adopted to combat malnutrition concerns the development of diversified diets. Indeed, the greater the diversity of a diet, the lower the risk that the diet is insufficient in terms of micronutrient supply, therefore understanding dietary patterns is important to plan the right approach to overcome hidden hunger. The main limit of this strategy is the difficulty of providing a balanced diet accessible to low-income populations.

Since it is not practicable either to provide diversified diets, or to adopt fortification and supplementation programs for the entire world population, staple crop biofortification is now the most concrete solution for addressing the problem of hidden hunger [8].

Biofortification focuses on enhancing the content of Fe, Zn, and vitamins in crops through agronomic practices, conventional breeding techniques or genetic modification.

The most common approach to improve micronutrient content in the edible parts of plants, and thus to increase human intake, is soil or foliar application of fertilizers. Although previous studies have revealed the successful application of this approach [15,16], results are dependent on crop and soil mineral availability. Moreover, the application is expensive, as fertilizers must be applied regularly, it is not possible to direct the micronutrients towards the edible parts and excessive usage of fertilizers can lead to environmental concerns.

With the need to overcome these limitations, attempts have been made to use genetic biofortification by exploiting the genetic variability of crops and conventional breeding techniques. To date, modern biotechnologies represent the most interesting perspective for biofortification. The transgenic approach appears to be the best option in cases where genetic variability is limited or absent. Furthermore, this approach allows to perform multiple genetic manipulations on a single organism to direct the accumulation of micronutrients towards the edible parts of plants [17–19].

In recent decades, scientific studies and initiatives such as HarvestPlus focused on iron, zinc and vitamin A biofortification because they are considered the most limited micronutrients according to the World Health Organization [13].

According to the HarvestPlus about 283 varieties of biofortified crops have been released so far in 30 countries among which: zinc wheat, rice and maize; vitamin A cassava, maize, sweet potato; iron bean and pearl millet (https://www.harvestplus.org/).

Some biofortified crops have been developed using non-transgenic techniques such as rice with enhanced Zn and Se content [20], wheat with higher Fe and Zn [21], or maize [22] and wheat enriched with provitamin A [6,23] and essential minerals [24].

Phytic acid, also known as InsP$_6$ or PA, is a naturally occurring compound found in many plant-based foods, including grains, legumes and nuts. PA can bind to minerals such as Ca, Fe, Zn, and Mg, lowering their availability for absorption in the human body [24,25]. Addressing the challenge of reducing or eliminating PA in cereals has led to the development of low phytic acid (*lpa*) mutants in major crops through various genetic strategies [26,27].

Several experiments were made to block PA biosynthesis by targeting different genes at various steps of the pathway. However, it was demonstrated that the disruption of the biosynthetic pathway at the early steps can affect the plant inositol metabolism and disturb related pathways. Therefore, the best strategies to develop *lpa* mutants seem to be represented by the silencing of PA biosynthesis genes involved in the final steps, such as the gene encoding the *inositol 1,3,4,5,6-pentakisphosphate 2-kinase* (*IPK1*) [28,29].

IPK1 is a member of inositol phosphate kinase superfamily. In plants, it is expressed in different tissues including seeds, roots, leaves and flowers and it is involved in various biological processes, such as stress response, gene regulation, and cell signalling [30,31]. IPK1 is crucial in regulating the PA synthesis in seeds, affecting the rate of PA accumulation during seed development [26,32]. Mutations in the *IPK1* gene have been shown to reduce the levels of phytic acid in seeds, also showing severe effects on plant growth and development. The silencing of the *IPK1* gene in rice and wheat through the RNAi approach led to the development of *lpa* mutants able to accumulate higher amount of Fe and Zn in the kernel [32,33]. Similar results were obtained in bread wheat by the silencing of *TaIPK1-A1* gene using CRISPR/Cas9 technology [29]. The analysis of the genome-edited lines revealed a significant decrease in the PA content accompanied by 1.5–2.1 fold increase in the Fe concentration and 1.6–1.9 fold rise in Zn concentration. Phenotypic analyses revealed an altered spike architecture in transgenic plants without compromising significantly grain yield [29].

The goal of the research here presented is the development of new durum wheat genotypes biofortified in essential minerals through the silencing of *TdIPK1* genes using a non-transgenic approach known as Targeting Induced Local Lesions in Genome (TILLING) [34].

2. Materials and methods

2.1. Isolation and phylogenesis of IPK1 sequences

In order to identify the sequence of *TdIPK1*, the orthologous genes of *Triticum aestivum* were used as a query and blasted against *Triticum turgidum* ssp *durum* cv. Svevo genome in Ensembl Plants database (https://plants.ensembl.org/index.html).

The IPK1 protein sequences of the major grass species were identified by blasting the protein sequences in NCBI BLASTP software (https://blast.ncbi.nlm.nih.gov/Blast.cgi) and the phylogenetic analysis was carried out by MEGA11 software [35]. The evolutionary history among the selected taxa were deduced using the Neighbor-Joining (NJ) method with the p-distance method and pairwise deletion option. The multiple sequence alignment of IPK1 proteins was performed by T-Coffee Expresso 11.0 tool (https://tcoffee.crg.eu/apps/tcoffee/do:expresso).

Secondary and tertiary structures of the TdIPK1 proteins were predicted using the GOR IV (https://npsa.lyon.inserm.fr/cgi-bin/npsa_automat.pl?page=/NPSA/npsa_gor4.html) and SWISS MODEL (https://swissmodel.expasy.org/) tools.

2.2. Plant materials

Two TdIPK1 mutant lines, deriving from the treatment with EMS mutagen, were identified through the platform WheatTILLING available at the University of Davis (https://dubcovskylab.ucdavis.edu/home) [36]. In detail, the lines Kronos 2700 and Kronos 1194 had a nonsense mutation in the exon II of the *TdIPK1-A1* homeoallele and in the exon IV of *TdIPK1-B1* homeoallele, respectively (Fig. S1). The two mutations were pyramided crossing the homozygous mutant lines (TdIPK1-A1⁻ and TdIPK1-B1⁻). The F$_1$ generation was self-pollinated and the selection of the different genotypes was conducted on the derived F$_2$ and F$_3$ progenies. The partial null mutants were grown in a controlled growth chamber with initial vernalization at 4–5 °C for 3 weeks, followed by 18–26 °C day and 16–18 °C night temperature with a 16 h light period along with the controls (cv. Kronos and wild-type sibling lines selected by the cross).

2.3. DNA extraction

Genomic DNA was extracted from leaves (F_2 progeny) and half seeds (F_3 progeny) using the NucleoSpin® Plant II (Macherey-Nagel) kit and according to the manufacturer's instruction. The DNA was used as template for the analysis of HRM-genotyping.

2.4. HRM analysis

HRM analysis was performed on the F_2 progeny of the cross TdIPK1-A1⁻ X TdIPK1-B1⁻. Amplicons were produced by a nested PCR strategy. The first PCR was carried out to amplify genome-specific fragments for *TdIPK1-A1* and *TdIPK1-B1* homeoalleles, respectively, using the primer pairs reported in Table S1. The reaction was performed in a 20 µl volume using the following conditions: 10 µl of 2X GoTaq® G2 Hot Start Colorless Master Mix (Promega, Madison, USA), 0.5 µM of each primer, 20 ng of template DNA and nuclease-free water up to 20 µl volume, with the following conditions: 95 °C for 2 min, followed by 38 cycles at 95 °C for 30 s, 56 °C for 30 s, 72 °C for 1 min and a final extension at 72 °C for 5 min. The first PCR reaction was diluted 60-fold and 2 µl were used as a template for the second PCR reaction for HRM analysis. The second reaction was carried out using the primer pairs reported in Table S1 and prepared as follows: 2 µl of diluted DNA template, 5 µl of 2X GoTaq® G2 Hot Start Colorless Master Mix (Promega), 0.5 µM of each primer, 1 µl LC Green Plus (Idaho Technology Inc., Salt Lake City, USA) and nuclease-free water up to 10 µl volume. The PCR program was carried out following these conditions: 95 °C for 2 min, followed by 39 cycles at 95 °C for 30 s, 60 °C for 20 s, 72 °C for 20 s and a final extension at 72 °C for 5 min. At the end of the final extension step, the reaction was held at 95 °C for 30 s, then at 25 °C for 1 min. The PCR reaction was carried out in 96-well Frame-Star plates (4titude Ltd., Surrey, UK) overlaid with 10 µl of mineral oil (Sigma-Aldrich, St. Louis, MO, USA), and the analyses of the melting curves was performed by the Light Scanner instrument (Idaho Technology, Inc.).

2.5. Analyses of the gene expression by quantitative real time PCR (qRT-PCR)

Immature seeds of the partial null mutants along with the control (cv. Kronos) at 14 Days Post Anthesis (DPA) were harvested, immediately frozen in liquid nitrogen and stored at –80 °C. Total RNA was extracted using the Spectrum Plant Total RNA kit (Sigma-Aldrich, St. Louis, USA) following manufacturer's instructions. One µg of the extracted RNA was used as template for the synthesis of cDNA, following the protocol indicated in the QuantiTect Reverse Transcription Kit (Qiagen, Hilden, Germany). The analyses of qRT-PCR were performed using the CFX 96 Real-TimePCR Detection System device (Bio-Rad Hercules, CA, USA). The reaction was prepared in a final volume of 10 µl containing the following concentrations: 5 µl of 2X SsoAdvUniver SYBR GRN SMX (Bio-Rad Hercules, CA, USA), 0.5 µM of each primer and 1 µl of cDNA. The qRT-PCR program had the following conditions: 95 °C for 3 min, followed by 39 cycles at 95 °C for 10 s and 60 °C for 30 s. A melting curve was generated over the range 75–95 °C, with 0.5 °C increments at 5 s/step. Transcript quantification was enabled by CFX manager software. Three biological replicates were analysed for each genotype, and each biological replicate was represented by three technical replicates. The list of genes analysed, along with the housekeeping β-actin gene, and the used primers are shown in Table S2.

2.6. Determination of PA and visualization of iron deposits

PA was determined as described in Frittelli et al. [24]. Briefly, mature seeds of selected F_4 partial mutant lines (TdIPK1-A1⁻, TdIPK1-B1⁻) along with the controls (cv. Kronos and WT sibling lines) were grounded to fine powder by a laboratory Cycline Mill (Cyclotec 1093, FOSS, Hilleröd, Sweden). PA was determined using a commercial

kit (K-PHYT kit, Megazyme Inc, Bray, Ireland) and the PA content was expressed in the form of mean values of three biological replicates ± standard error. Three technical replicates were carried out for each biological replicate. A one-way analysis of variance and the post hoc Tukey's HSD test (p-value< 0.05) were used to identify significant differences among mean values.

The ferric iron (Fe^{3+}) deposits were stained in F_4 mature seeds of the same genotypes as described in Frittelli et al. [24], with Perls' blue staining method [37,38] and a stereo microscope was used to assess the staining intensity.

2.7. Determination of macro- and micro-nutrient

Mature F_4 seeds of the selected mutant lines along with controls (cv. Kronos) were grounded to fine powder and oven-dried at 80 °C. As described in Frittelli et al. [24], samples were introduced in polypropylene tubes (digiTUBES, SCP Science, Champlain, NY, USA). After the addition of 3 mL of concentrated nitric acid and 1 mL of concentrated hydrogen peroxide, samples were heated in a block system (DIGIPREP, SCP Science, Champlain, NY, USA) at 95 °C for 2 h. The extracts were then filtered by a 0.45 µm teflon filter (DigiFILTER, SCP Science, Champlain, NY, USA). The digests were diluted with dH_2O and analysed by inductively coupled plasma-mass spectrometry (ICP-MS 7900, Agilent Technologies, Santa Clara, CA, USA) with Octopole Reaction System (ORS). Phosphorous and sulfur in the digested solutions were determined by inductively coupled plasma-optical emission spectrometer (ICP-OES 5100 Agilent Technologies, Santa Clara, CA, USA) using the operating conditions described in Frittelli et al. [24]. Data were expressed as mean values of three biological replicates ± standard error and three technical replicates were carried out for each biological replicate.

2.8. Root analysis of IPK1 mutants

The root systems of the selected TdIPK1 mutant lines along with control plants (cv. Kronos and WT sibling lines) were analysed to highlight any morphological differences. Mature seeds of F_4 progeny were left to germinate for 5 days in the dark at room temperature in Petri dishes. After germination, seedlings were transferred to a plastic pot filled with 2 L of a continuously aerated nutrient solution and were placed in a growth chamber under 27/20 °C and 14/10 h day/night cycles with a relative humidity of 80 % and 200 mmol m⁻² s⁻¹ PAR at leaf level for 5 days [39]. Roots were cut from the stem and placed in a Perspex tray with a film of water to reduce root overlapping. The WinRHIZO™ scanning equipment and software (EPSON1680, WinRHIZO Pro2003b Software; Regent Instruments Inc., Quebec, Canada) was employed to determine morphological root traits, such as volume and surface area, total root length, root diameter and number of root tips. Data were expressed as mean values of three technical replicates for three biological replicates ± standard error.

2.9. Field trial evaluation of yield-related traits

The experimental field trial was carried out at CREA-CI (Foggia, Italy) during the 2021–2022 growing season using standard agronomic practices. Cultivar Kronos and the mutant TdIPK1-B1⁻ genotypes were seeded in single plots, consisting of 1-m rows, 30 cm apart, with 30 germinating seeds per plot, and following a randomized complete block design with three replications. Plots were hand-harvested at maturity. The following yield-related traits were recorded from randomly selected spikes: Spike weight, Spike length, Spikelets number per spike, Kernels per spike and Kernel weight per spike.

2.10. Seed germination and seedling emergence rate

The germination rate was evaluated putting three replicas of seeds

(each with 50 units) to germinate in Petri dishes on layer of filter paper watered with the same volume. The Petri dishes were placed in an incubator with a temperature of 20 ℃ and relative humidity of 70 % during the whole germination test. Germination rate was estimated after a week according to the following equation: {[numer seed geminated]/ [total seed]}x 100.

Seedling emerge rate was determined in growing chamber (16/8 h day/night at 20 °C day/16 °C night). Seeds were sown at a depth of 30 mm and the seedlings were counted 15 days after sowing. The rate was expressed as the percentage of emerged seedlings.

3. Results

3.1. Phylogenesis of IPK1 proteins

With the aim to evaluate the evolutionary history of IPK1 enzymes in the major cereals and the model species *Arabidopsis thaliana*, a phylogenetic analysis was performed using MEGA11 software. A blast search of *TaIPK1-A1* (TraesCS2A02G497700) and *TaIPK1-B1* (TraesCS2B02G525900) run against the durum wheat genome in Ensembl Plants showed a high identity with TRITD2Av1G270440 and TRITD2Bv1G233570, respectively annotated as *TdIPK1-A1* and *TdIPK1-B1*. The IPK1 protein sequences used in phylogenetic tree were identified by blasting the protein sequences in NCBI BLASTP software. The phylogenetic analysis highlighted that TdIPK1 proteins were evolutionally close to *Triticum aestivum*, *Aegilops tauschii*, *Triticum dicoccoides*, *Hordeum vulgare*, *Brachypodium distachyon* and *Lolium rigidum*. Among the considered sequences, a second cluster was constituted by the IPK1 proteins isolated from *Oryza sativa*, *Oryza glaberrima*, *Zea mays*, *Panicum hallii* and *Setaria italica* (Fig. 1).

The multiple sequence alignment performed using T-Coffee Expresso tool showed a high level of identity among the sequences confirming the conservation of typical motifs among the species analysed (Fig. S2). TdIPK1 proteins had four typical motifs (GEG(G/A) ANL, RxxMHQxLK, LDxLDIEGx4Y, and EXKPK) (reported in bold letter in Fig. S2) that are strongly conserved in wheat, rice and maize species as already reported in previous works [32,40].

Despite the high level of identity among the sequences and the conservation of typical motifs, the two TdIPK1 proteins showed structural differences in the N-terminal and C-terminal regions that can explain a different biological activity (Fig. S3).

3.2. Selection of TdIPK1 mutants

With the objective of obtaining new genotypes with a lower content of phytic acid able to accumulate a higher content of essential minerals in the grain, a TILLING strategy was implemented to silence both the *TdIPK1* homeoalleles. Single null mutants in the two homeoalleles (*TdIPK1-A1* and *TdIPK1-B1*) were selected in the Wheat TILLING platform available at the University of Davis and the mutations were pyramided by crossing the two selected mutant lines. The mutations were followed in F_2 progeny of the cross (29 lines) through HRM-genotyping (Fig. S4). No double null mutants for the *TdIPK1* genes were identified in the F_2 generation. The analyses were, therefore, conducted on F_3 progenies of genotypes homozygous null mutants for one homeoallele and heterozygous for the second one. A total of 249 seeds were analysed, of which only two complete null mutants, out of 62 expected for a Mendelian segregation, were identified and confirmed by sequencing. Since the selected double null mutants demonstrated poor germination as well as difficulties in plant growth and development, these plants were unable to reach complete maturity and seed production.

Following the molecular screening, 46 and 68 single null lines TdIPK1-A1⁻ and TdIPK1-B1⁻ respectively, were selected (Table S3) and subsequently characterized together with the controls (cv. Kronos and wild-type sibling lines selected by the cross).
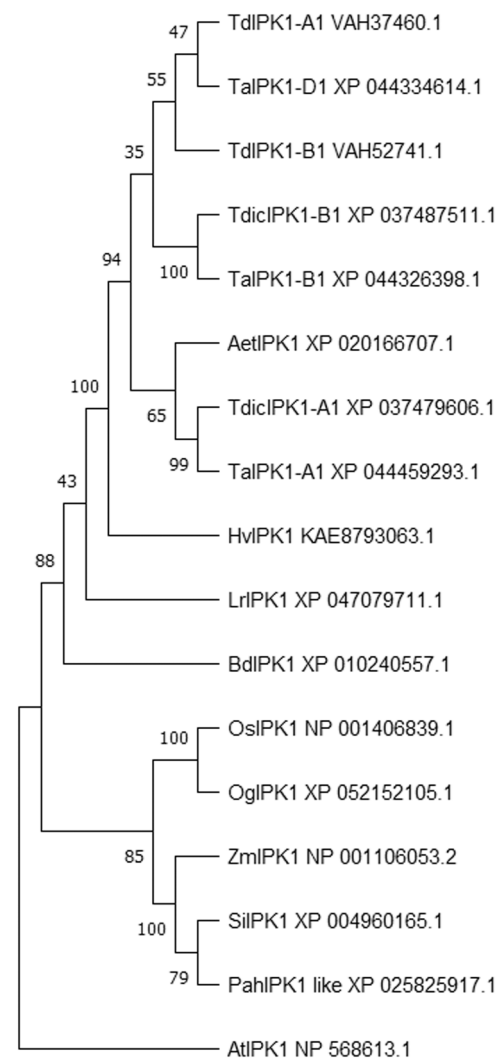

Fig. 1. Phylogenetic tree of IPK1 proteins in different plant species. At: *Arabidopsis thaliana* IPK1 (NP_568613.1); Lr: *Lolium rigidum* IPK1 like (XP_047079711.1); Og: *Oryza glaberrima* IPK1 (XP_052152105.1); Os: *Oryza sativa Japonica Group* IPK1 (NP_001406839.1); Pah: *Panicum hallii* IPK1 (XP_025825917.1); Bd: *Brachypodium distachyon* IPK1 (XP_010240557.1); Hv: *Hordeum vulgare* IPK1 (KAE8793063.1); Aet: *Aegilops tauschii* subsp. *strangulata* IPK1 (XP_020166707.1); Tdic: *Triticum dicoccoides* IPK1-A1 like (XP_037479606.1), IPK1-B1 like (XP_037487511.1); Ta: *Triticum aestivum* IPK1-A1 (XP_044459293.1), IPK1-B1 (XP_044326398.1), IPK1-D1 (XP_044334614.1); Td: *Triticum durum* ssp. *durum* IPK1-A1 (VAH37460.1); IPK1-B1 (VAH52741.1); Zm: *Zea mays* IPK1 (NP_001106053.2); Si: *Setaria italica* IPK1 (XP_004960165.1). The phylogenetic tree was constructed by the Neighbor-joining (NJ) method with pairwise deletion option and p-distance matrix in MEGA XI [35]. Bootstrap values (1000 replicates) were shown at each node.

3.3. Expression analysis of key genes involved in PA biosynthetic pathway

The expression analyses performed on the single homeoalleles (*TdIPK1-A1* and *TdIPK1-B1*) revealed a significant down-regulation (>70 %) of the two targeted genes in TdIPK1-A1⁻ and TdIPK1-B1⁻ mutant lines, respectively (Fig. 2). A significant reduction (>50 %) of transcript level in the two single null IPK1 mutant lines was also observed using the primer pair generic for *IPK1*.

To investigate if the silencing of the single homeoalleles can cause pleiotropic effects on the expression of the major genes involved in PA biosynthetic pathway, qRT-PCR was carried out on the mRNA (extracted from immature grain at 14 DPA) of the three genotypes (Kronos wild-
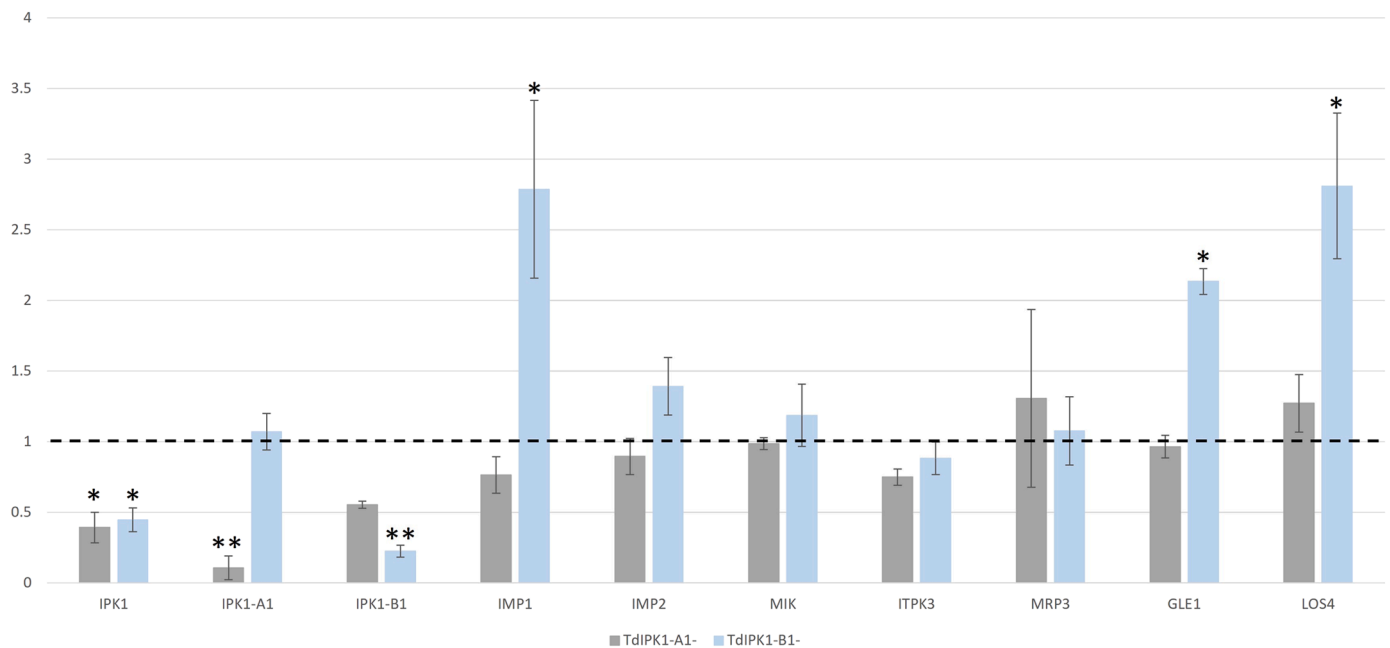
Fig. 2. Relative expression of TdIPK1 mutant lines compared to the control Kronos wild-type. The levels of gene expression were determined in relation to the transcription levels of the housekeeping gene β-actin. Data are expressed in the form of fold differences between the transcript abundance of the Kronos wild-type and the two TdIPK1 mutant lines (TdIPK1-A1⁻ and TdIPK1-B1⁻) for each gene considered for the analysis: *IMP, MIK; ITPK3; MRP3; Gle1; LOS4*. The bar graph represents the mean of three biological replicates, each one made of three technical replicates. The dotted line indicates the relative transcription value of the control Kronos wild-type. Standard error is indicated above each bar. Two-tailed Student's t-tests showed relative expression values with significant (*$p \leq 0.05$) and highly significant (**$p \leq 0.01$) differences compared to the control.

type, TdIPK1-A1⁻ and TdIPK1-B1⁻).

In detail, the expression analyses were performed on the following genes: *inositol monophosphate phosphatase* (*IMP*), involved in the production of free myo-inositol (Ins) from myo-inositol 3-phosphate (Ins(3)P₁); *myo-inositol kinase* (*MIK*), involved in the first phosphorylation step, consisting in the conversion of Ins to InsP₁; *inositol 1,3,4-triphosphate 5/6-kinase* (*ITPK*), involved in the phosphorylation of InsP₃ to InsP₅. In addition, the expression level of a non-biosynthetic gene, encoding the multidrug-resistance associated proteins 3 (MRP3), was investigated. This gene encodes a vacuolar transmembrane protein involved in the transport and storage of PA in the vacuole. The data showed that the silencing of the *IPK1* genes in the TdIPK1-A1⁻ and TdIPK1-B1⁻ mutants did not determine changes in the expression levels of the analysed genes, except for the *IMP1* gene that resulted up-regulated (2.8 fold) in TdIPK1-B1⁻ mutant lines (Fig. 2).

To unveil the molecular basis behind the presumed lethality associated with the *IPK1* gene mutation in our double null genotype, we choose to examine the expression of a dual protein functional complex known to be activated by the binding of the InsP6 cofactor and involved in essential processes such as mRNA nuclear export at the nuclear pore complex and translational initiation and termination at the cytosol. The two protein Gle1 and LOS4 works in the paradigm Gle1-InsP6-LOS4 where the cofactor binding to Gle1 activate the ATPase/RNA helicase LOS4 [41,42]. Here, the expression analysis revealed an up-regulation of both *Gle1* (2.1 fold) and *LOS4* (2.8 fold) in the TdIPK1-B1⁻ mutants compared to TdIPK1-A1⁻ and control Kronos (Fig. 2).

3.4. Biochemical characterization of TdIPK1 mutants

The analysis of PA content revealed significant differences among the controls (cv. Kronos and WT sibling lines) and the partial null mutant genotypes (TdIPK1-A1⁻ and TdIPK1-B1⁻) selected from the F₃ segregating progenies grown in the field at the Experimental Farm of University of Tuscia in the season 2022–2023. In detail, PA content was reduced by about 19 % and 17 % in the TdIPK1-A1⁻ and TdIPK1-B1⁻

mutants, respectively (Fig. 3). No difference was found comparing the Kronos wild-type with the F₃ wild-type sibling lines.

Since PA acts as a chelator of essential mineral cations, the modulation of PA accumulation in seeds can be associated with an increased bioavailability of nutrients.

The Perls assay carried out on longitudinal sections of mature caryopses highlighted an increase in iron deposits in both the mutant lines compared to the control. In this regard, the intensity of stained Fe increased in the scutellum and aleuronic layers of the TdIPK1-A1⁻ and TdIPK1-B1⁻ single null homozygous mutants (Fig. 4).

Macro- and micro-nutrient contents were found altered in our mutant genotypes (Fig. 5). Concerning macronutrients, an increase of Mg (+60 %), P (+40 %) and S (+25 %) was observed in the TdIPK1-B1⁻ mutant compared to the control Kronos. Differently, the TdIPK1-A1⁻ mutant presented a greater accumulation for K (+20 %), whereas the other macronutrients were not differentially accumulated. Noteworthy, the grain of TdIPK1-B1⁻ contained a significantly higher content of important microelements compared to the control Kronos wild-type, i.e. Fe (+72 %), Mn (+30 %) and Zn (+126 %) contents.

3.5. Agronomic performance and roots morphological analyses

The agronomic performances of TdIKP1-B1⁻ mutant were measured in the field by evaluating a set of yield-related parameters compared to the control cv. Kronos. Significant differences were registered for Spike weight (–14 %), Spike kernel weight (–17 %), Single kernel weight (–12 %), seed germination rate (–23.4 %) and seedling emergence rate (–43.4 %) which were lower in the TdIPK1-B1⁻mutant genotype compared to the control (Fig. 6; Table S4). No difference was observed for Spike length, Spikelets number per spike and Kernels per spike (Fig. 6).

To evaluate if the silencing of *IPK1* genes affected the root architecture, the root apparatus of the set of selected mutant lines was analysed by measuring root length, root surface area, volume, diameter and number of root tips (Fig. 7). No differences were found for all measured parameters comparing the single null mutants TdIPK1-A1⁻ and TdIPK1-
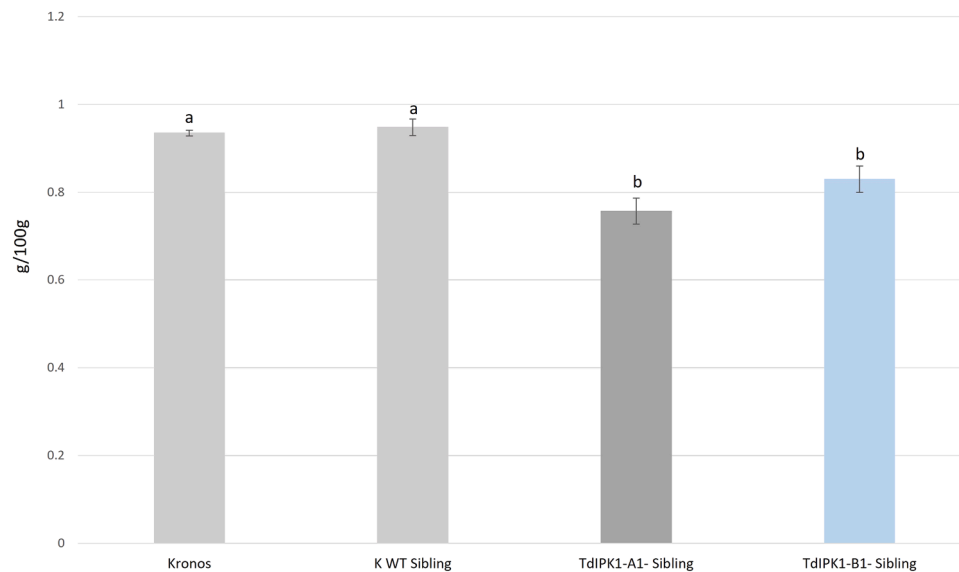
Fig. 3. Determination of phytic acid (PA) content in *lpa* mutants along with the control genotypes (cv. Kronos and K WT sibling lines). Mean values of three biological replicates, error bars indicate standard errors. Values followed by different letters differ significantly from one another (one-way ANOVA, Tukey HSD test, $p < 0.05$).
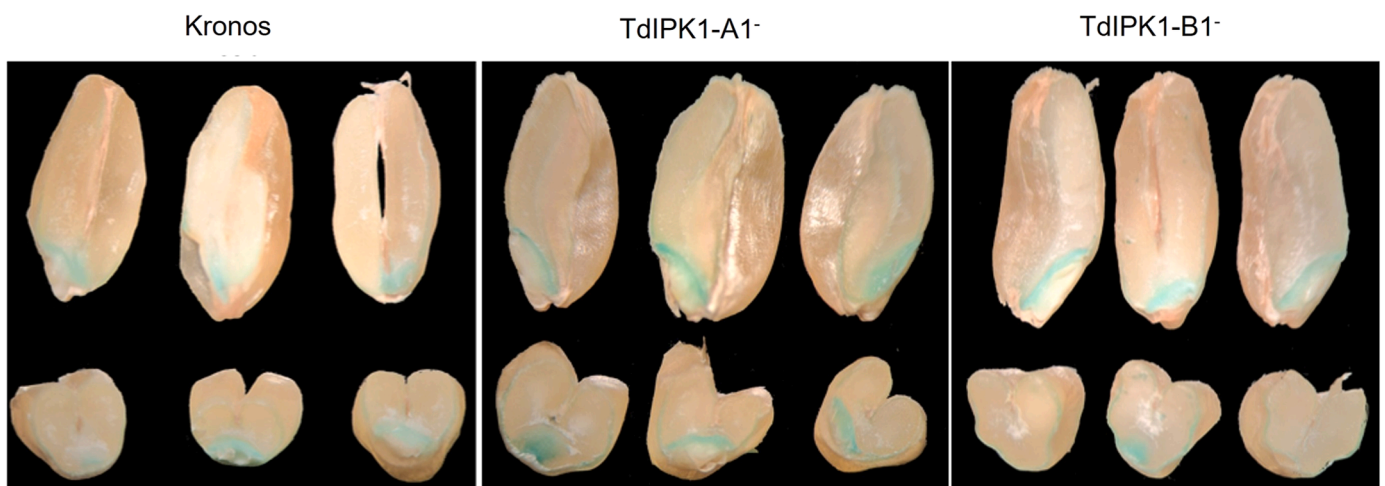

Fig. 4. Localization of Fe deposits within the kernel with Perls' blue staining. The image shows the longitudinal (top) and the transversal sections (bottom), of the seeds of cv. Kronos, TdIPK1-A1⁻, TdIPK1-B1⁻.

B1⁻ to the control plants (Kronos wild-type) (Fig. 7).

4. Discussion

Micronutrient deficiencies affect 3 billion people, leading to serious health, economic and social consequences especially in low- and middle-income countries [3]. Since it is unrealistic to fight malnutrition only through a balanced and varied diet for the entire world population, the biofortification of staple crops represents the most valid solution [8].

Although durum wheat kernels are rich in micronutrients, their bioavailability in semolina is limited due to the presence of anti-nutritional compounds [43]. Among them, PA [InsP₆] is one of the major anti-nutrients limiting the micronutrient bioavailability in durum wheat. In fact, PA is a strong chelator of cations important for nutrition such as Ca, Fe, Zn, and Mg, making them less available for the body absorption. Therefore, to address the issue of low nutrient bioavailability, the modulation of PA in seeds and the development of *lpa* mutants represent valid strategies for micronutrients biofortification. In this paper, we focused on the silencing of *inositol 1,3,4,5,6-pentakisphosphate*

2-kinase (*IPK1*), a member of inositol phosphate kinase superfamily. In literature, it has been reported that the suppression of this gene is one of the most effective methods for developing *lpa* crops [29,32,33].

In detail, the research here presented focused on the development and characterization of durum wheat genotypes where *TdIPK1* genes were silenced through a TILLING approach.

In silico analysis of TdIPK1 proteins showed phylogenetic closeness among cultivated and wild wheat and the major crops in the following order: *T. durum*, *T. dicoccoides*, *T. aestivum*, *Ae. tauschii*, barley, *L. rigudum*, *B. distachyon*. More divergence was observed for *Zea mays*, *P. hallii*, *S. italica* and rice. The comparison of IPK1 amino acid sequences confirmed the high degree of conservation of proteins among plant species. The phylogenetic analysis regrouped in the same cluster wheat, barley, *L. rigidum* and *B. distachyon* confirming high relatedness among these species as previously reported [6,23,40]. These results agree also with the study of Wicker et al. [44], which demonstrated that gene structure, order and content are highly conserved between barley and wheat providing evidence of a parallel evolution of their genome. The multiple sequence alignment performed using T-Coffee Expresso tool
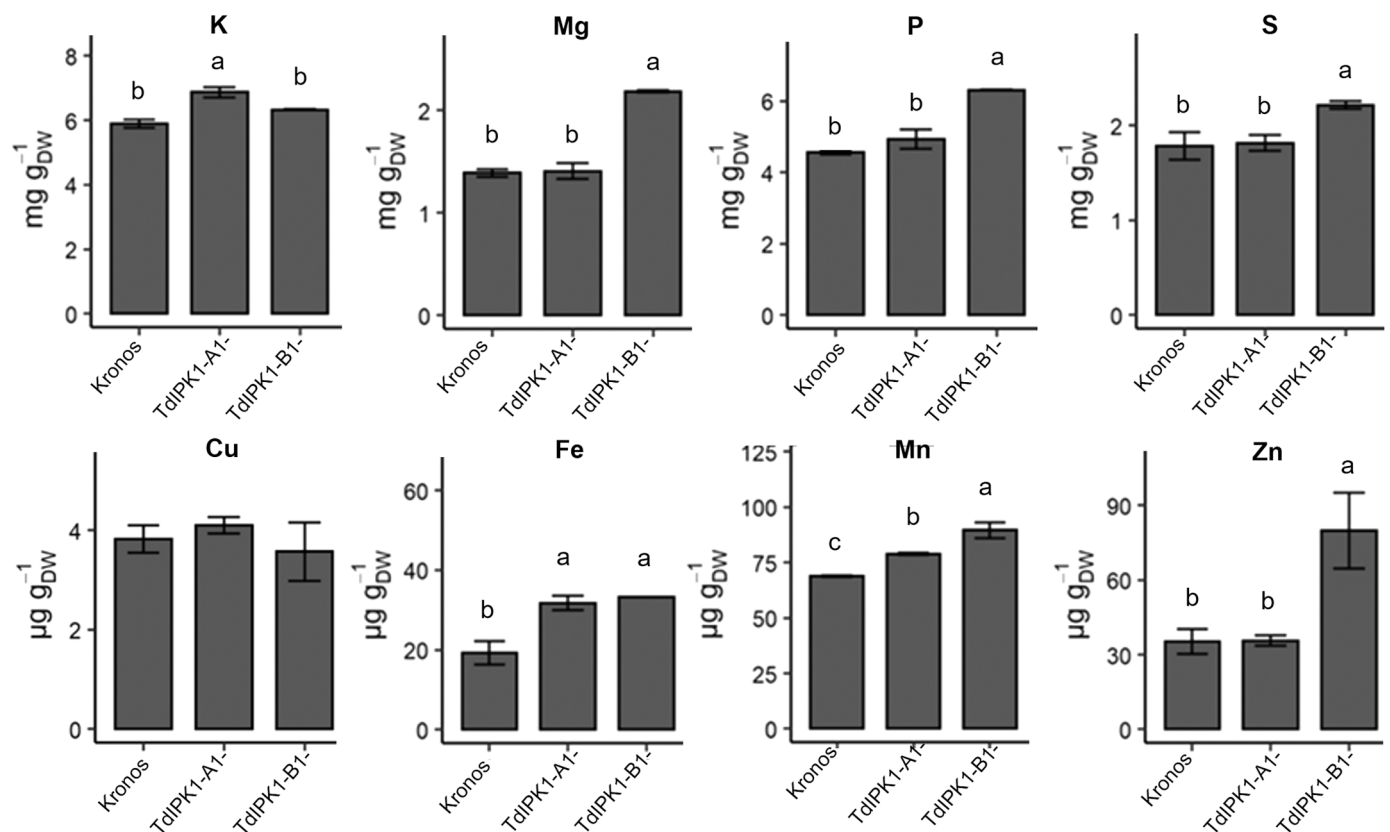
Fig. 5. Concentration of macro-and micro-nutrients in *lpa* mutants and Kronos wild-type kernels. Mean values of three biological replicates ± Dev. St. One-way ANOVA, LSD post hoc test, $p < 0.05$.

confirmed the conservation of typical motifs among wheat, rice and maize species as previously reported by Ali et al. [32] and Bhati et al. [40].

The unexpected pattern of segregation, along with the poor germination of the two complete *null* TdIPK1 lines here identified, suggests that *TdIPK1* genes have an essential role for pollen fertility, seed formation or plant development. Almost all *lpa* mutations, described during the last decades, were associated with negative pleiotropic effects regarding germination frequency, seedling emergence, seed viability and plant development [30,45–48] confirming that PA plays key roles in essential plant developmental processes [49]. In bread wheat, the expression of *TaIPK1* homeoalleles was modulated either through a transgenic approach or genome editing, but in no cases a full suppression of this gene was reported, suggesting a crucial role in plant development and growth [29,32,33]. In this regard, Ali et al. [32] reduced *IPK1* transcripts of 3.8-fold in T4 RNAi transgenic lines; Aggarwal and colleagues [33] obtained similar results using the same technique.

As expected, the expression analyses performed on *TdIPK1-A1* and *TdIPK1-B1* genes revealed that there is a significant down-regulation of the target genes in TdIPK1-A1⁻ and TdIPK1-B1⁻ mutant lines, respectively, confirming that the presence of premature stop codons on the two *IPK1* homeoalleles affects their expression level. The degradation of nonfunctional transcripts is due to the activation of a mechanism of quality control preventing the accumulation of truncated proteins, which is known as nonsense-mediated decay (NMD) [50]. Similar results were already observed in durum wheat TILLING mutants [23,51]. The investigation of the main PA biosynthetic genes did not detect significant pleiotropic effects at gene expression level in the immature grain of the two mutant lines, except for *IMP1* which was strongly up-regulated in the TdIPK1-B1⁻ mutants. IMP1 plays an important role in many metabolic and signalling pathways in plants. Besides being essential for the de novo synthesis of myo-inositol, and for recycling of Ins in Ins (1,4,

5) P₃, it also is involved in ascorbic acid synthesis, indicating a bifunctionality that links these two branches of carbon metabolism [52]. Karmakar et al. [53] found an up-regulation of *IMP1* in RNAi rice lines where the *ITP5/6 K-1* gene was downregulated. They speculated that the down-regulation of the *ITP5/6 K-1* gene produced an accumulation of Ins3 (P), responsible for the pathway shifting toward the reversible steps catalysed by the *IMP1* and *MIPS* (*myo-inositol-3-phosphate synthase*) genes to synthesize myo-inositol through the lipid-dependent pathway.

In addition to its role as a reservoir for phosphate, InsP₆ has been associated to key cellular processes such as mRNA export, translational control, RNA editing and DNA repair in yeast, mammals and more recently in plants [41].

The involvement of InsP6 in such essentially biological processes well fits with our finding of the double null IPK1 lethal phenotype. For this purpose, we examined the expression profile of a protein complex implicated in mRNA transport and processing, Gle1-LOS4, reported to be activated by InsP6 [41]. InsP₆ acts as a cofactor linking and stabilizing the Gle1-LOS4 interaction by binding to a pocket at the interface between Gle1 and LOS4 [41]. The same authors demonstrated that the expression of *Gle1* variant with enhanced InsP₆ sensibility stimulated the expression of *LOS4* rescuing the defects in mRNA export identified in IPK1 InsP₆ deficient mutants. Here, the expression analyses performed on *Gle1* and *LOS4* genes revealed an up-regulation of these genes in TdIPK1-B1⁻ mutants. The drastic reduction of *TdIPK1-B1* transcript levels (–78 % compared to the control) due to the silencing of *TdIPK1-B1* homeoallele seems to activate the expression of both genes (*Gle1* and *LOS4*) suggesting the existence of a causal relationship with the diminished availability of InsP6 in the lower PA content mutant line. The engineering of the Gle1 PA pocket has been proposed as a possible approach to improve the agronomic performances of *lpa* mutants.

The significant reduction of the PA content in the mature grain was accompanied by an increase of Fe depositions in the scutellum and
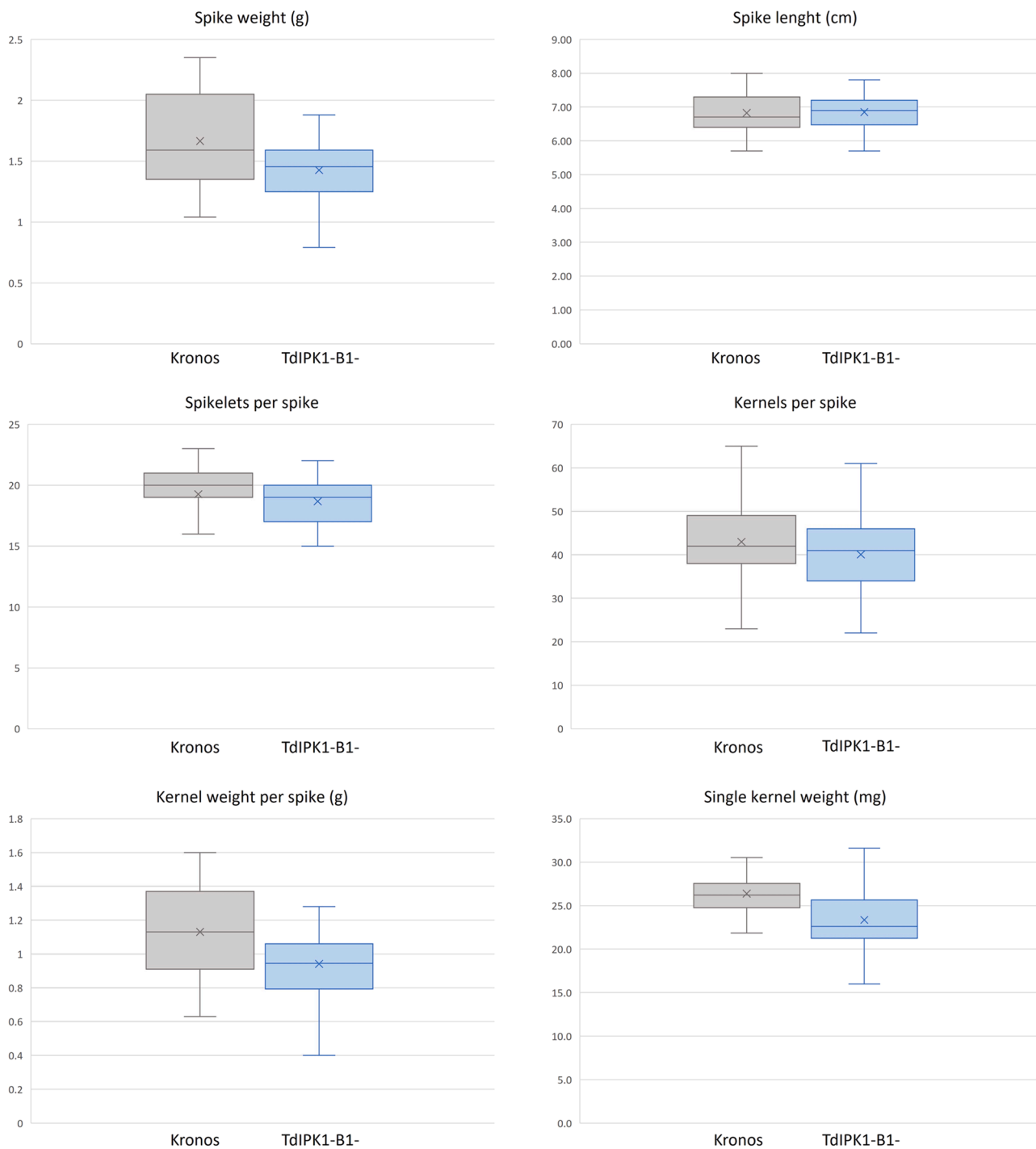
Fig. 6. Analyses of agronomical yield-related traits of TdIPK1-B1⁻ mutants compared to the control Kronos wild-type.

aleuronic layer in both single null homozygous mutants. This observation was confirmed by the increase of some macro and micronutrients in the TdIPK1 mutant kernels (overall in the single null TdIPK1-B1⁻) compared to the controls. In detail, TdIPK1-B1⁻ lines showed an increase in macronutrients, such as Mg (+60 %), P (+40 %) and S (+25 %), and micronutrient as Fe (+72 %), Mn (+30 %) and Zn (+126 %) contents.

The deeper change detected in the mineral profile of TdIPK1-B1⁻ mutant suggests a different functionality between the isoforms coded by the two homoeoalleles; this hypothesis is supported by the observation of significant variances in the predicted spatial conformation of the two enzymes (TdIPK1-A1 and TdIPK1-B1) (Fig. S3). Further, the substantial increase in micronutrient concentration compared to the relative more

modest variation in PA level could be due to an overestimation of PA levels in our mutants. This overestimation could be attributed to the method that also detects inositol phosphate intermediates, resulting from the blockage of the final PA biosynthetic step.

Previous studies performed on bread wheat revealed similar results. In detail, the silencing of *TaIPK1* genes through RNAi strategy led to an increase in Fe (1.2–1.7-fold), and Zn (1.3–2.2-fold) [33]. The increase in micronutrients content was accompanied by a drastic reduction of PA (–56 % in RNAi mutant lines). Analysis of a set of TaIPK1-A1 genome-edited lines revealed a significant decrease in the PA (–72 %) content accompanied by 1.5–2.1 fold increase in the Fe concentration and 1.6–1.9 fold rise in Zn [29]. A similar behaviour, but more modest,
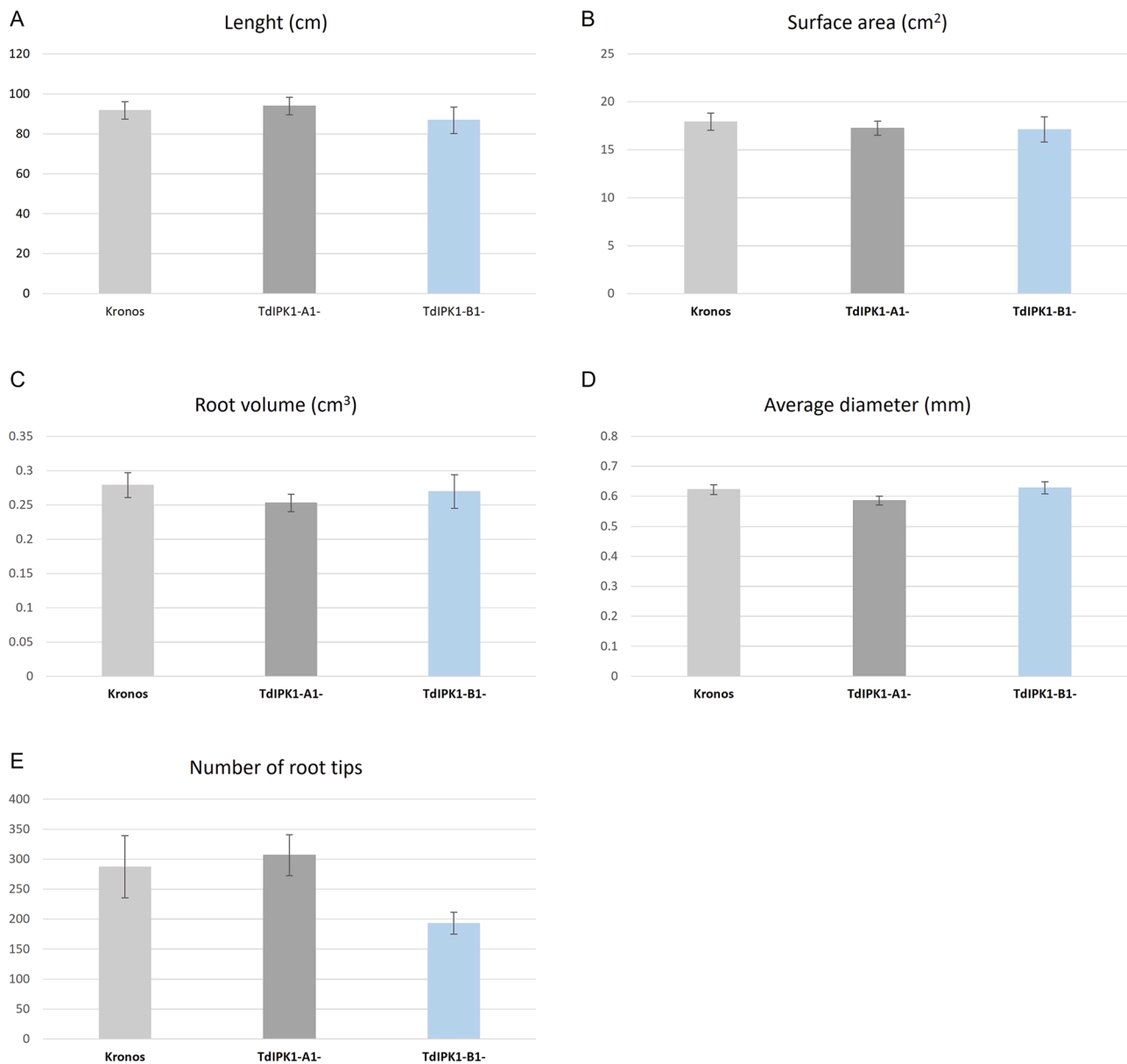
Fig. 7. Root morphological traits: length (A), surface area (B), volume (C), diameter (D) and number of root tips (E) in *lpa* mutants and cv. Kronos. Mean values of three biological replicates ± St. Err. One-way ANOVA, LSD post hoc test, $p < 0.05$.

was observed in the single null TdIPK1 mutant lines.

The *lpa* mutants described in Aggarwal et al. [33] and Ibrahim et al. [29] showed less drastic pleiotropic effects in terms of germinability, and yield compared to other studies [27,28], probably due to a partial silencing of the gene. The agronomical analyses along with the seed germination and seedling emergence rate performed on the TdIPK1-B1⁻ genotypes revealed pleiotropic yield-related traits associated with the *TdIPK1* silencing in contrast to what was observed in rice and *Arabidopsis thaliana* where the IPK1 silencing did not affect the seed development [32,54]. According to Aggarwal et al. [33], the silencing of the *TdIPK1* homealleles determined a significant reduction in Spike weight, Kernel weight per spike and Single kernel weight. However, no alterations in spike architecture were observed as previously found in genome edited lines produced by Ibrahim et al. [29]. Finally, both single null TdIPK1 mutant lines did not exhibit significant differences for all measured root characteristics compared to the wild type, suggesting that the TdIPK1 silencing did not affect the exploitation potential of the root system.

5. Conclusion

Although the transgenic approach has been found to be a powerful tool for mineral biofortification [29,33], genetically modified organisms are still subjected to law restrictions which limit their cultivation, processing and marketing. In this work, the use of TILLING strategy allowed to develop non GM durum wheat lines potentially useful in future biofortification breeding programs without legal restrictions. Our results demonstrated that *Td-IPK1-B1* has a main role compared to its homeo-allele (*Td-IPK1-A1*), as only the suppression of the former has produced a genotype able to accumulate higher amounts of micronutrients in the grain. Our study suggests that the complete absence of both homeoallele is lethal for plant development. The introduction of Gle1 variants could be a successful strategy in future breeding programs to mitigate the pleiotropic effects caused by the complete suppression of this gene.

Authors' contributions

FS conceived the work, coordinated and supervised the activities. FS and MV acquired the funding. AF, SC, GQ and PDV curated investigation and data. SA, FS and SP validated data. AF and FS wrote the original draft. SA, SM, PDV, EB and SP revised and edited the manuscript. All authors contributed to the article and approved the submitted version.

Funding

Declaration of Competing Interest

The authors declare that they have no known competing financial interests or personal relationships that could have appeared to influence the work reported in this paper.

Data Availability

The data that has been used is confidential.

Acknowledgements

Appendix A. Supporting information

Supplementary data associated with this article can be found in the online version at doi:10.1016/j.cpb.2023.100309.

References

[1] N.M. Lowe, The global challenge of hidden hunger: perspectives from the field, Proc. Nutr. Soc. 80 (3) (2021) 283–289.
[2] K. Von Grebmer, A. Saltzman, E. Birol, D. Wiesman, N. Prasai, S. Yin,Y. Yohannes, P. Menon, J. Thompson, A. Sonntag, 2014. Synopsis: 2014 global hunger index: The challenge of hidden hunger (Vol. 83). Intl Food Policy Res Inst.
[3] FAO, IFAD, UNICEF, WFP, and WHO, 2019. The State of Food Security and Nutrition in the World 2019. Safeguarding Against Economic Slowdowns and Downturns. Rome: FAO. Available online at: http://www.fao.org/3/ca5162en/ca5162en.pdf.
[4] S. Muthayya, J.H. Rah, J.D. Sugimoto, F.F. Roos, K. Kraemer, R.E. Black, The global hidden hunger indices and maps: an advocacy tool for action, PloS One 8 (6) (2013), e67860.
[5] S. Lockyer, A. White, J.L. Buttriss, Biofortified crops for tackling micronutrient deficiencies–what impact are these having in developing countries and could they be of relevance within Europe? Nutr. Bull. 43 (4) (2018) 319–357.
[6] F. Sestili, M.D. Garcia-Molina, G. Gambacorta, R. Beleggia, E. Botticella, P. De Vita, D.V. Savatin, S. Masci, D. Lafiandra, Provitamin A biofortification of durum wheat through a TILLING approach, Int. J. Mol. Sci. 20 (22) (2019) 5703.
[7] Vitamin and Mineral Nutrition Information System (VMNIS), 2022. Available at: https://www.who.int/teams/nutrition-and-food-safety/databases/vitamin-and-mineralnutrition-information-system (Accessed December 2023).
[8] S. Sheoran, S. Kumar, V. Ramtekey, P. Kar, R.S. Meena, C.K. Jangir, Current status and potential of biofortification to enhance crop nutritional quality: an overview, Sustainability 14 (6) (2022) 3301.
[9] J. Thompson, B.A. Biggs, S.R. Pasricha, Effects of daily iron supplementation in 2- to 5-year-old children: systematic review and meta-analysis, Pediatrics 131 (4) (2013) 739–753.
[10] S.R. Pasricha, M. Low, J. Thompson, A. Farrell, L.M. De-Regil, Iron supplementation benefits physical performance in women of reproductive age: a systematic review and meta-analysis, J. Nutr. 144 (6) (2014) 906–914.
[11] A.L. Stammers, N.M. Lowe, M.W. Medina, S. Patel, F. Dykes, C. Perez-Rodrigo, L. Serra-Majam, M. Nissensohn, V.H. Moran, The relationship between zinc intake and growth in children aged 1–8 years: a systematic review and meta-analysis, Eur. J. Clin. Nutr. 69 (2) (2015) 147–153.
[12] E. Liu, L. Pimpin, M. Shulkin, S. Kranz, C.P. Duggan, D. Mozaffarian, W.W. Fawzi, Effect of zinc supplementation on growth outcomes in children under 5 years of age, Nutrients 10 (3) (2018) 377.
[13] World Health Organization, Guidelines on food fortification with micronutrients, World Health Organization,, 2006.
[14] R. Olson, B. Gavin-Smith, C. Ferraboschi, K. Kraemer, Food fortification: the advantages, disadvantages and lessons from sight and life programs, Nutrients 13 (4) (2021) 1118.
[15] Y. Ludwig, I.H. Slamet-Loedin, Genetic biofortification to enrich rice and wheat grain iron: from genes to product, Front. Plant Sci. 10 (2019), 833.
[16] Y. Ramzan, M.B. Hafeez, S. Khan, M. Nadeem, S. Batool, J. Ahmad, Biofortification with zinc and iron improves the grain quality and yield of wheat crop, Int. J. Plant Prod. 14 (2020) 501–510.
[17] P.J. White, M.R. Broadley, Biofortification of crops with seven mineral elements often lacking in human diets–iron, zinc, copper, calcium, magnesium, selenium and iodine, N. Phytol. 182 (1) (2009) 49–84.
[18] M. Garg, N. Sharma, S. Sharma, P. Kapoor, A. Kumar, V. Chunduri, P. Arora, Biofortified crops generated by breeding, agronomy, and transgenic approaches are improving lives of millions of people around the world, Front. Nutr. 5 (2018), 12.
[19] A. Kiran, A. Wakeel, K. Mahmood, R. Mubaraka, S.M. Haefele, Biofortification of staple crops to alleviate human malnutrition: contributions and potential in developing countries, Agronomy 12 (2) (2022) 452.
[20] A.V.D.J. Mangueze, M.F. Pessoa, M.J. Silva, A. Ndayiragije, H.E. Magaia, V. S. Cossa, F.H. Reboredo, M.L. Carvalho, J.P. Santos, M. Guerra, A.I. Ribeiro-Barros, F.C. Lidon, J.C. Ramalho, Simultaneous zinc and selenium biofortification in rice. Accumulation, localization and implications on the overall mineral content of the flour, J. Cereal Sci. 82 (2018) 34–41.
[21] S.K. Verma, S. Kumar, I. Sheikh, S. Malik, P. Mathpal, V. Chugh, S. Kumar, R. Prasad, H.S. Dhaliwal, Transfer of useful variability of high grain iron and zinc from Aegilops kotschyi into wheat through seed irradiation approach, Int. J. Radiat. Biol. 92 (3) (2016) 132–139.
[22] P. Manjeru, A. Van Biljon, M. Labuschagne, The development and release of maize fortified with provitamin A carotenoids in developing countries, Crit. Rev. Food Sci. Nutr. 59 (8) (2019) 1284–1293.
[23] M.D. Garcia Molina, E. Botticella, R. Beleggia, S. Palombieri, P. De Vita, S. Masci, D. Lafiandra, F. Sestili, Enrichment of provitamin A content in durum wheat grain by suppressing β-carotene hydroxylase 1 genes with a TILLING approach, Theor. Appl. Genet. 134 (2021) 4013–4024.
[24] A. Frittelli, E. Botticella, S. Palombieri, S. Masci, S. Celletti, M.C. Fontanella, S. Astolfi, P. De Vita, M. Volpato, F. Sestili, The suppression of TdMRP3 genes reduces the phytic acid and increases the nutrient accumulation in durum wheat grain, Front. Plant Sci. 14 (2023) 46.
[25] H.W. Lopez, F. Leenhardt, C. Coudray, C. Remesy, Minerals and phytic acid interactions: is it a real problem for human nutrition? Int. J. Food Sci. Technol. 37 (7) (2002) 727–739.
[26] F. Sparvoli, E. Cominelli, Seed biofortification and phytic acid reduction: a conflict of interest for the plant? Plants 4 (4) (2015) 728–755.
[27] V. Raboy, Low phytic acid crops: observations based on four decades of research, Plants 9 (2) (2020) 140.
[28] F. Colombo, D. Paolo, E. Cominelli, F. Sparvoli, E. Nielsen, R. Pilu, MRP transporters and low phytic acid mutants in major crops: main pleiotropic effects and future perspectives, Front. Plant Sci. 11 (2020), 1301.
[29] S. Ibrahim, B. Saleem, N. Rehman, S.A. Zafar, M.K. Naeem, M.R. Khan, CRISPR/Cas9 mediated disruption of Inositol Pentakisphosphate 2-Kinase 1 (TaIPK1) reduces phytic acid and improves iron and zinc accumulation in wheat grains, J. Adv. Res. 37 (2022) 33–41.
[30] H.F. Kuo, T.Y. Chang, S.F. Chiang, W.D. Wang, Y.Y. Charng, T.J. Chiou, Arabidopsis inositol pentakisphosphate 2–kinase, AtIPK1, is required for growth and modulates phosphate homeostasis at the transcriptional level, Plant J. 80 (3) (2014) 503–515.
[31] E. Riemer, N.J. Pullagurla, R. Yadav, L. Hansjosten, R. Priyanshi, H.J. Jessen, M. Kamleitner, G. Schaaf, D. Laha, Regulation of plant biotic interactions and abiotic stress responses by inositol polyphosphates, Front. Plant Sci. 2835 (2022).
[32] N. Ali, S. Paul, D. Gayen, S.N. Sarkar, S.K. Datta, Development of low phytate rice by RNAi mediated seed-specific silencing of inositol 1, 3, 4, 5, 6-pentakisphosphate 2-kinase gene (IPK1), PloS One 8 (7) (2013), e68161.
[33] S. Aggarwal, A. Kumar, K.K. Bhati, G. Kaur, V. Shukla, S. Tiwari, A.K. Pandey, RNAi-mediated downregulation of inositol pentakisphosphate kinase (IPK1) in wheat grains decreases phytic acid levels and increases Fe and Zn accumulation, Front. Plant Sci. 9 (2018), 259.
[34] C.M. McCallum, L. Comai, E.A. Greene, S. Henikoff, T argeting I nduced L ocal L esions IN G enomes (TILLING) for plant functional genomics, Plant Physiol. 123 (2) (2000) 439–442.
[35] K. Tamura, G. Stecher, S. Kumar, MEGA11: molecular evolutionary genetics analysis version 11, Mol. Biol. Evol. 38 (7) (2021) 3022–3027.
[36] K.V. Krasileva, H.A. Vasquez-Gross, T. Howell, P. Bailey, F. Paraiso, L. Clissold, J. Simmonds, R.H. Ramirez-Gonzalez, X. Wang, P. Borrill, C. Fosker, S. Ayling, A. L. Phillips, C. Uauy, J. Dubcovsky, Uncovering hidden variation in polyploid wheat, Proc. Natl. Acad. Sci. 114 (6) (2017) E913–E921.
[37] S. Krishnan, G.A.I. Ebenezer, P. Dayanandan, Histochemical localization of storage components in caryopsis of rice (Oryza sativa L.), Curr. Sci. (2001) 567–571.
[38] C. Prom-u-Thai, B. Dell, G. Thomson, B. Rerkasem, Easy and rapid detection of iron in rice grain, ScienceAsia 29 (2003) 203–207.
[39] G. Quagliata, S. Abdirad, S. Celletti, F. Sestili, S. Astolfi, Screening of Triticum turgidum genotypes for tolerance to drought stress, Plant Physiol. Biochem. 194 (2023) 271–280.

[40] K.K. Bhati, S. Aggarwal, S. Sharma, S. Mantri, S.P. Singh, S. Bhalla, J. Kaur, S. Tiwari, J.K Roy, R. Tuli, A.K. Pandey, Differential expression of structural genes for the late phase of phytic acid biosynthesis in developing seeds of wheat (Triticum aestivum L.), Plant Sci. 224 (2014) 74–85.

[41] H.S. Lee, D.H. Lee, H.K. Cho, S.H. Kim, J.H. Auh, H.S. Pai, InsP6-sensitive variants of the Gle1 mRNA export factor rescue growth and fertility defects of the ipk1 low-phytic-acid mutation in Arabidopsis, Plant Cell 27 (2) (2015) 417–431.

[42] B. Montpetit, N.D. Thomsen, K.J. Helmke, M.A. Seeliger, J.M. Berger, K. Weis, A conserved mechanism of DEAD-box ATPase activation by nucleoporins and InsP6 in mRNA export, Nature 472 (7342) (2011) 238–242.

[43] V. Raboy, Approaches and challenges to engineering seed phytate and total phosphorus, Plant Sci. 177 (4) (2009) 281–296.

[44] T. Wicker, S. Taudien, A. Houben, B. Keller, A. Graner, M. Platzer, N. Stein, A whole-genome snapshot of 454 sequences exposes the composition of the barley genome and provides evidence for parallel evolution of genome size in wheat and barley, Plant J. 59 (5) (2009) 712–722.

[45] S.J. Meis, W.R. Fehr, S.R. Schnebly, Seed source effect on field emergence of soybean lines with reduced phytate and raffinose saccharides, Crop Sci. 43 (4) (2003) 1336–1339.

[46] M. Guttieri, D. Bowen, J.A. Dorsch, V. Raboy, E. Souza, Identification and characterization of a low phytic acid wheat, Crop Sci. 44 (2) (2004) 418–424.

[47] R. Pilu, M. Landoni, E. Cassani, E. Doria, E. Nielsen, The maize lpa241 mutation causes a remarkable variability of expression and some pleiotropic effects, Crop Sci. 45 (5) (2005) 2096–2105.

[48] X.H. Xu, H.J. Zhao, Q.L. Liu, T. Frank, K.H. Engel, G. An, Q.Y. Shu, Mutations of the multi-drug resistance-associated protein ABC transporter gene 5 result in reduction of phytic acid in rice seeds, Theor. Appl. Genet. 119 (2009) 75–83.

[49] S.B. Shears, Assessing the omnipotence of inositol hexakisphosphate, Cell. Signal. 13 (3) (2001) 151–158.

[50] P.A. Frischmeyer, H.C. Dietz, Nonsense-mediated mRNA decay in health and disease, Hum. Mol. Genet. 8 (10) (1999) 1893–1900.

[51] F. Sestili, S. Palombieri, E. Botticella, P. Mantovani, R. Bovina, D. Lafiandra, TILLING mutants of durum wheat result in a high amylose phenotype and provide information on alternative splicing mechanisms, Plant Sci. 233 (2015) 127–133.

[52] J. Fu, K. Peterson, M. Guttieri, E. Souza, V. Raboy, Barley (Hordeum vulgare L.) inositol monophosphatase: gene structure and enzyme characteristics, Plant Mol. Biol. 67 (2008) 629–642.

[53] A. Karmakar, S. Bhattacharya, S. Sengupta, N. Ali, S.N. Sarkar, K. Datta, S.K. Datta, RNAi-mediated silencing of ITPK gene reduces phytic acid content, alters transcripts of phytic acid biosynthetic genes, and modulates mineral distribution in rice seeds, Rice Sci. 27 (2020) 315–328.

[54] J. Stevenson-Paulik, R.J. Bastidas, S.T. Chiou, R.A. Frye, J.D. York, Generation of phytate-free seeds in Arabidopsis through disruption of inositol polyphosphate kinases, Proc. Natl. Acad. Sci. 102 (35) (2005) 12612–12617.